# CHAPTER VI

# FIELD EXPERIMENTS AND DATA COLLECTION

## 6.1 MEASUREMENT OF SOIL PROPERTIES

### 6.1.1 Soil classification

Before the field tests, soil samples were randomly collected from the test plot for classification. The sieve analysis method was used to classify the soil according to the USDA textural triangle for soil classification (McKyes, 1989). The soil on the test plot was found to be classified as sandy loam containing 19% clay, 12% silt and 69% sand.

### 6.1.2 Soil density, soil water content and cone index

Different spots in the test plot were randomly selected for collecting soil samples by applying a cylindrical soil sampler of 60 mm diameter and 100 mm long which was forced into the soil surface and rotated to cut the soil sample. The soil samples were oven dried and the dried bulk density and the soil water content determined. In total ten samples were collected for each soil condition and the average of the readings, as well as other soil characteristics, are shown in Table 6.1.

The cone index was also measured to quantify the soil strength profile for reference purpose. The aim was to ensure that the soil strength was relatively uniform in the treatment areas. The average cone index for the range of depths to 400 mm was recorded for each penetration. The measurement was repeated ten times for each soil condition. The average values for the measurements and the standard deviations obtained were accepted as the final cone index and is shown in Table 6.1.

Table 6.1 Soil physical properties and other field conditions for the field tests

| Field number | Soil classification | Surface coverage | Bulk density (dry basis, kg/m$^3$) | Soil water content (dry basis, %) | Average cone index (kPa) | Standard deviation for CI (kPa) |
|---|---|---|---|---|---|---|
| 1 | Sandy loam | None | 1126 | 7.8 | 433 | 28 |
| 2 | Sandy loam | None | 1245 | 13.3 | 675 | 45 |
| 3 | Sandy loam | None | 1310 | 21 | 745 | 43 |

## 6.2 EXPERIMENTAL PROCEDURE FOR SOIL CHARACTERIZATION

### 6.2.1 Pressure-sinkage characterization for the test plot

The original bevameter technique, without considering the slip sinkage, according to the procedure proposed by Wong (1989, 1993) as reviewed in Chapter 2, was adapted in this research to obtain the soil parameters in equation (2.1). The parameters $k_c$, $k_\phi$ and n, were derived according to the method described by Wong (1989, 1993).

The instrumented test device and the sinkage plates, as described in Chapter 5, were used for soil characterization. Each of the three sinkage plates with dimensions as explained in Chapter 5, was loaded to penetrate into the soil at approximately 25 mm/s, as recommended by Wong (1989, 1993). The pressure-sinkage curves for the three soil water content conditions are shown in Figure 6.1 to Figure 6.3. The results of the sinkage tests were analyzed by applying the pressure-sinkage relationship equation proposed by Bekker (1958, 1965) and the values of $k_c$, $k_\phi$ and n determined.

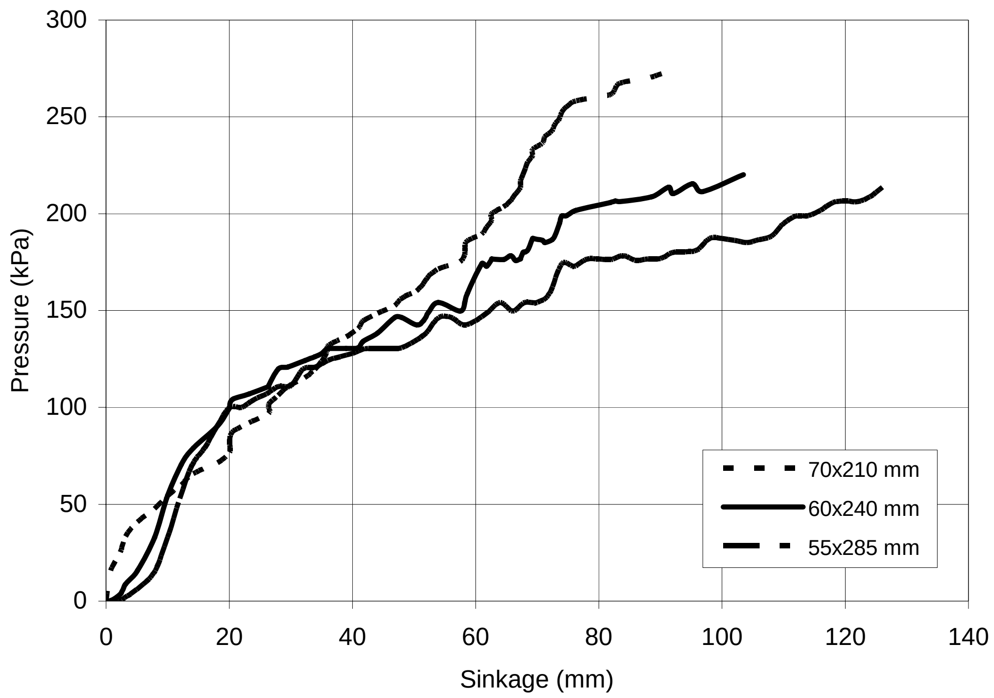


Figure 6.1. Contact pressure-sinkage curves for the sandy loam soil with soil water content 7.8% (dry basis).

The values of $k_c$, $k_\phi$ and n were calculated based on the results of at least two tests with two plates having different widths by plotting the p-z curves on log-log scale resulting in two parallel straight lines of the same slope. The proposed procedure by Wong (1989, 1993) was adapted to obtain values for the sinkage parameters.

The pressure-sinkage characteristics obtained from the measurements are shown in Table 6.2.

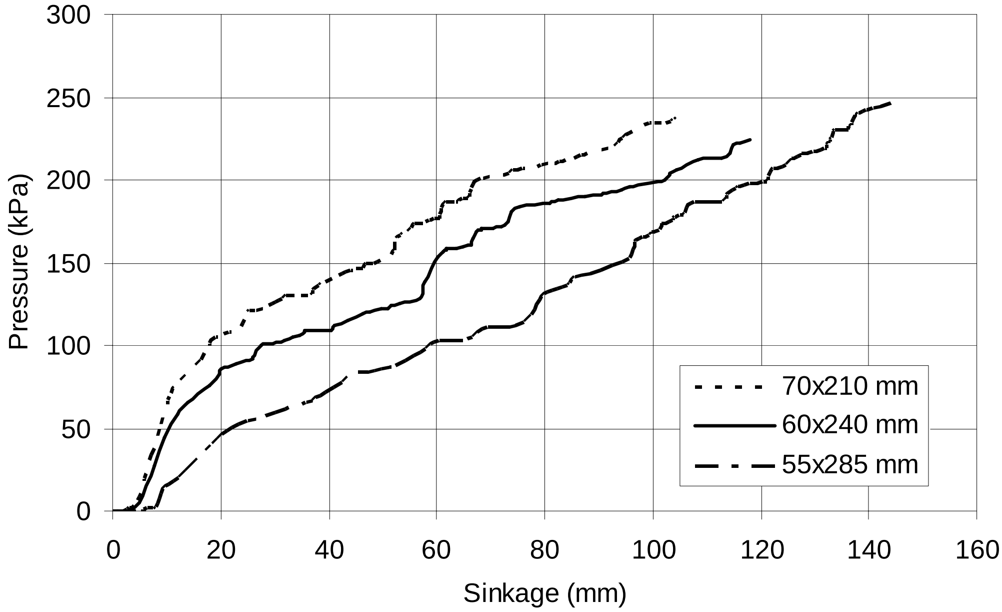


Figure 6.2. Contact pressure-sinkage curves for the sandy loam soil with soil water content 13.3% (dry basis).

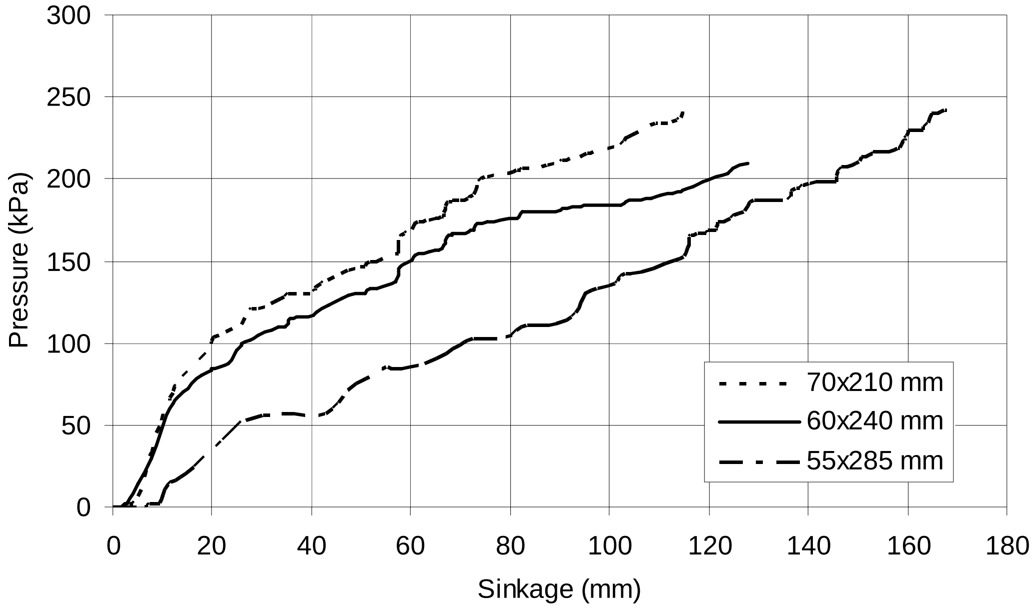


Figure 6.3. Contact pressure-sinkage curves for the sandy loam soil with soil water content 21% (dry bassis).

Table 6.2. Sinkage parameters obtained from pressure-sinkage tests.

| Soil water content (dry basis, %) | $k_c$, ($kN/m^{n+1}$) | $k_\phi$, ($kN/m^{n+2}$) | n |
|---|---|---|---|
| 7.8 | 37.9 | 1520 | 0.91 |
| 13.3 | 56.6 | 1630 | 0.89 |
| 21 | 54.1 | 1890 | 0.93 |

To simulate the unloading and reloading of the contact load exerted by the track, repetitive pressure-sinkage tests were also carried out in the field. The repetitive loading tests were performed following the same procedure as for the conventional sinkage tests. The sinkage plate penetrated into the soil up to a specified depth and then the load was slowly reduced to zero. The plate was reloaded to obtain the original depth for the sinkage tests. The curves for the applied vertical load vs vertical sinkage are shown in Figure 6.4.

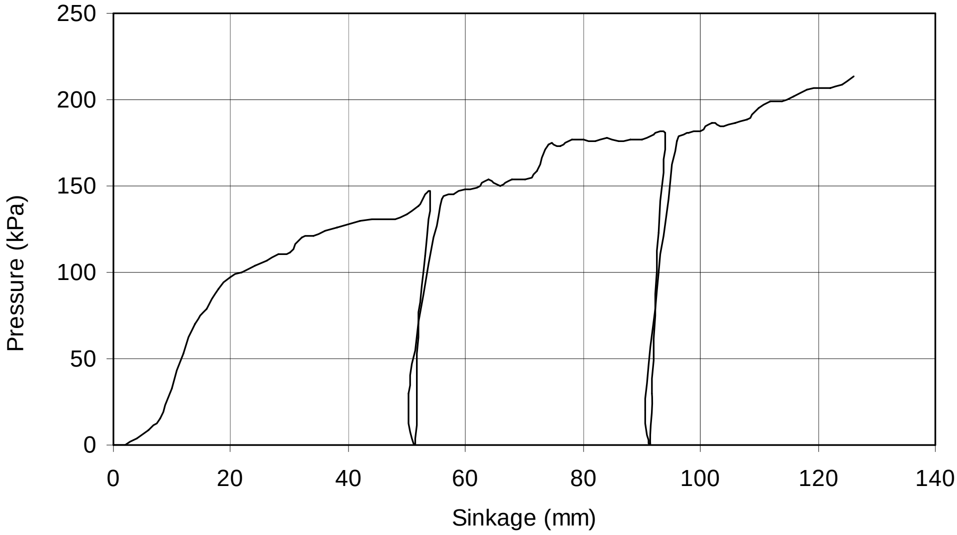


Figure 6.4. The loading/reloading curves for a sinkage tests (Sinkage plate: 60mmx240mm. Soil type: sandy loam. Soil water content=21%).

To apply the characterization for traction modelling, the related parameters, as suggested by Wong (pp. 38-44, 1989; pp. 115-125, 1993) could be used.

### 6.2.2 Soil-rubber frictional and soil shear characterization

To simulate the shape of the ground track contact area, the rectangular steel shear plates were used to determine the soil shear characteristics.

The investigation was initially carried out to measure soil parameters using a steel shear grouser and soil-rubber frictional characteristics by testing a track element removed from the prototype integral track assembly. The test results indicated that the shape of the soil shear stress-displacement curves and the values of the frictional characteristics for the rubber to soil interface were notably different from those obtained by the soil-soil shear caused by steel grousers (Figure 6.5 and Figure 6.6). It was shown that under the soil conditions tested, the shear curves obtained with the steel shear grouser exhibited the characteristics that the shear stress initially increased rapidly and reached a maximum value of shear stress at a particular shear displacement, and then decreased and approached a constant residual value for further shear displacement (Figure 6.5). This phenomenon can well be expressed by the equation (2.5) as reviewed in Chapter 2. The internal soil shear characteristics obtained from the field tests are shown in Table 6.3.

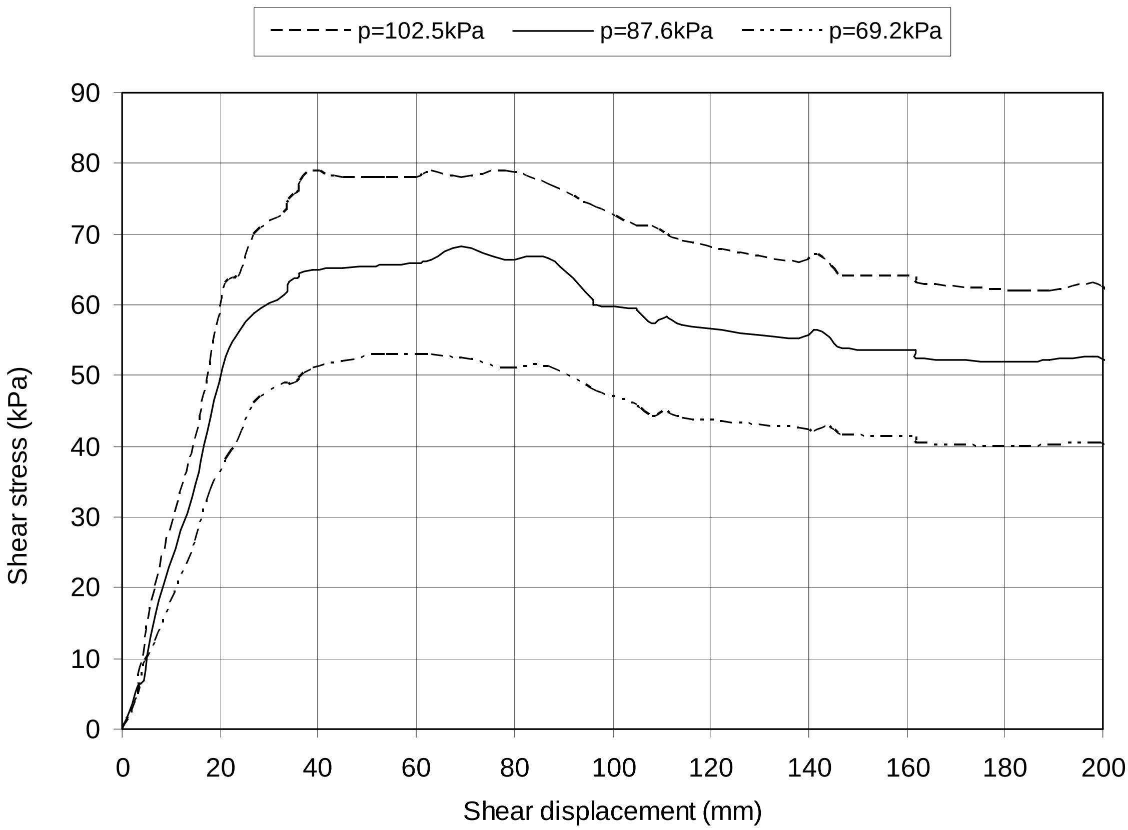


Figure 6.5. Shear curves for a soil shear test using a steel shear grouser (Soil type: sandy loam. Soil water content=7.8%).

Table 6.3. Internal soil shear characteristics from the tests.

| Field No | Soil water content dry basis, (%) | Cohesion c, (kPa) | Soil internal friction angle $\phi$, (deg) | Shear displacement $K_\omega$ at maximum shear stress, (m) |
|---|---|---|---|---|
| 1 | 7.8 | 3.13 | 38.5 | 0.029 |
| 2 | 13.3 | 3.65 | 37 | 0.035 |
| 3 | 21 | 2.79 | 30 | 0.031 |

On the other hand, the friction-shear curves obtained with the rubber track element exhibited the characteristic that the friction-shear stress initially increased rapidly with an increase in corresponding displacement, and approached a constant value with a further increase in displacement (Figure 6.6 through Figure 6.8). This can better be fitted by an equation similar to equation (2.6) as proposed by Janosi and Hanamoto (1963). However, the contact surface of the prototype track with rubber surface was smooth without grousers penetrating into soil. It was, therefore, more reasonable that the rationale might be explained that the tangential thrust was mainly due to the friction between the rubber and the terrain surfaces, rather than the internal friction of the soil. The rubber-soil adhesion also replaced the soil-soil cohesion for conventional soil shear characterization. Consequently, the test results for traction modelling using a track element with a smooth rubber surface was better related to the actual situation than the steel shear grousers.

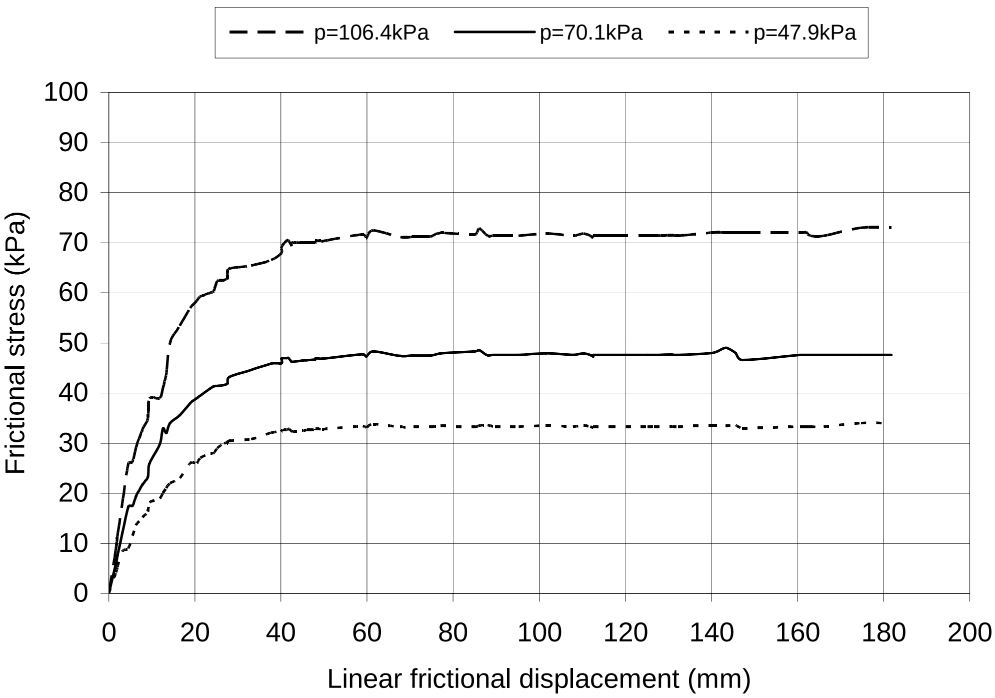


Figure 6.6. Friction curves for rubber-soil friction test (Soil type: sandy loam. Soil water content=7.8%).

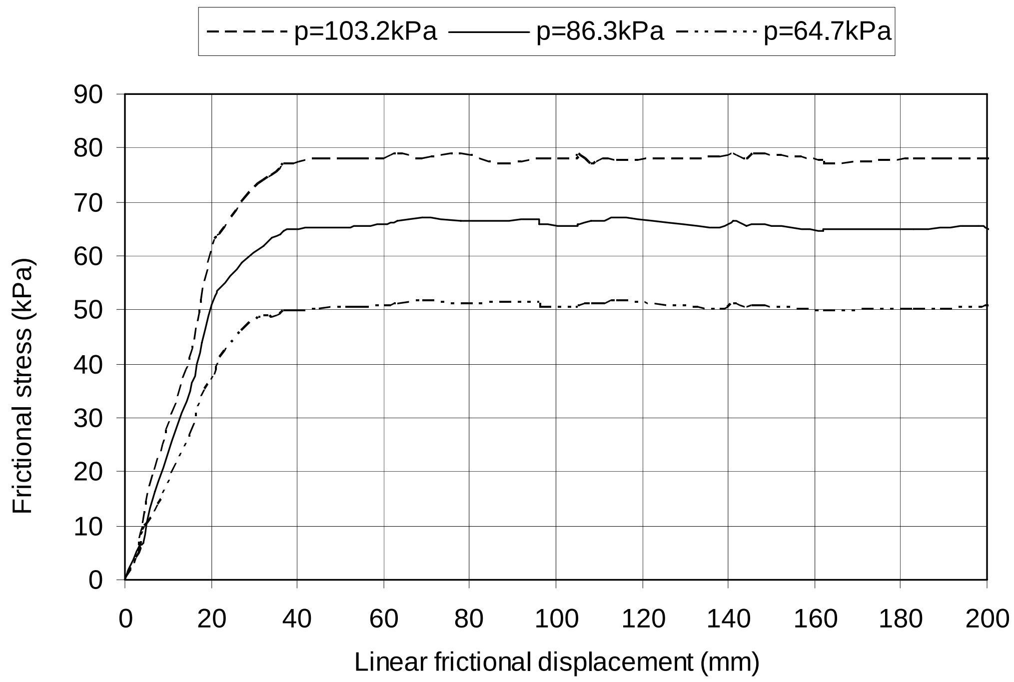


Figure 6.7. Friction curves for rubber-soil friction test (Soil type: sandy loam. Soil water content=13.3%).

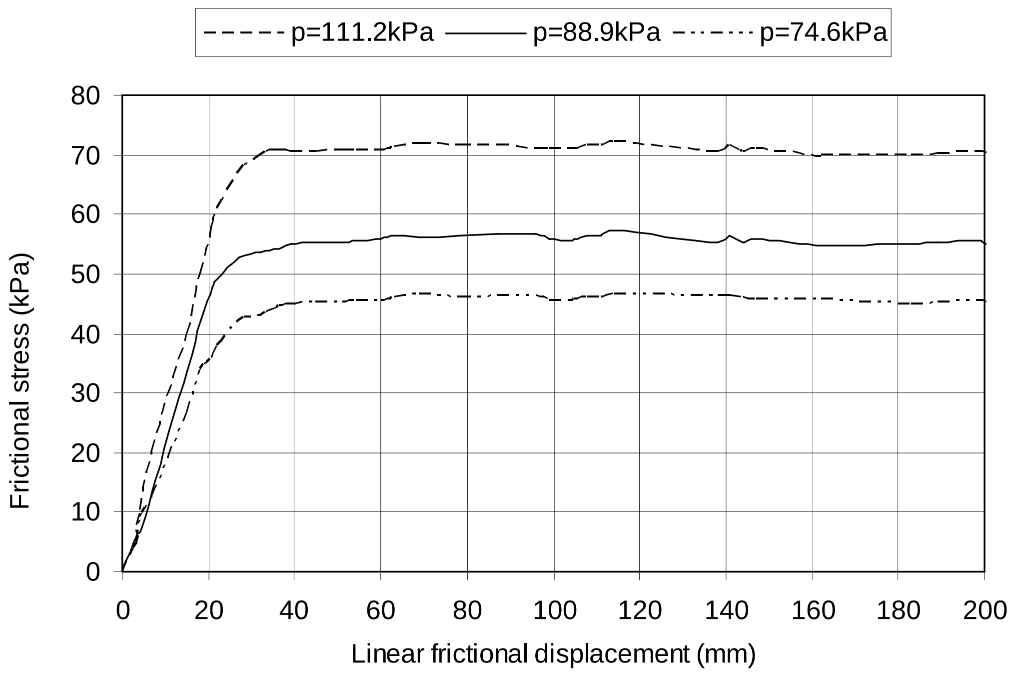


Figure 6.8. Friction curves for rubber-soil friction test (Soil type: sandy loam. Soil water content=21%).

For in situ test field measurements, ten frictional tests were conducted for each soil condition. The test results were then chosen to be analyzed by applying equation (4.2). The final results are shown in Table 6.4.

Table 6.4. Soil-rubber frictional characteristics from the tests.

| Field No | Soil water content, dry basis (%) | Rubber-terrain adhesion $c_a$, (kPa) | Angle of rubber-terrain friction δ, (degree) | Frictional deformation modulus K, (mm) |
|---|---|---|---|---|
| 1 | 7.8 | 1.89 | 33 | 28.5 |
| 2 | 13.3 | 2.96 | 36 | 28.8 |
| 3 | 21 | 2.49 | 32 | 27.8 |

The results as shown in Table 6.14 proved that the rubber-soil adhesion was much smaller than the soil-soil cohesion, whilst the angle of rubber-soil friction was very similar to the angle of soil internal friction. This tendency corresponds with data as reported by Neal (1966).

## 6.3 DRAWBAR PULL TESTS AND DATA COLLECTION

Full scale drawbar pull tests were conducted in the field to verify the traction models. During the drawbar pull tests, the parameters related to the distribution of the contact pressure and tangential stress per track element were also measured by the extended octagonal ring transducers. All the drawbar pull tests were conducted at relatively low speed ranges.

At the commencement of each test run, the tested tractor with the track and the loading tractor or tractors behind were properly leveled in both lateral and longitudinal directions to ensure the correct recording of the drawbar pull. The tow bar for the drawbar load was adjusted to be parallel to the ground surface. All the instrumentation was also finally checked or calibrated if necessary for correct function. The sampling frequency for recording the data was set at 60 samples per second, based on the previous field experience and the comprehensive consideration for system response and the real time accuracy of data recording. This resulted in ten recorded samples per second for each signal channel.

Before the data was recorded, the travel speeds of the tested crawler and the loading tractor or tractors behind were steadily adjusted whilst the parameters to be measured were observed by computer monitoring in the tractor cab. As soon as the observed values of the speeds or slip and the drawbar load reached desired values, data recording was triggered for all channels. Each test run was carried out applying the same procedure.

The recording time for each test run lasted ten seconds. The test for each set of the slip and the drawbar pull values was carried out until at least six seconds of smooth and steady readings were obtained and was then repeated three times. These readings recorded for six seconds were accepted as effective readings recorded and used for further processing and final analysis. The whole test was repeated three times.